

# Instrumental Aspects of Force Microscopy

Useful information for users of force microscopes

- some basic knowledge about AFM in general
- calibration procedures for piezoelectric scanners
- calibrations of normal and lateral forces

## 1- Cantilevers

### *i- Contact*

Scanning force microscopy is based on the measurement of the force between the probing tip and the sample, where the probing tip is attached to a cantilever-type spring. Thus, the force acting on the probing tip will elastically deform the cantilever.

For shortness, the combination of cantilever and probing tip is referred to as the “cantilever” or “lever”. If the spring constant  $c_B$  is known, the net force  $F$  can be derived directly from the deflection  $\Delta z$  according to the equation

$$F = c_B \cdot \Delta z \quad (1)$$

## ii- Non-contact

With a weak spring of 0.1N/m and a deflection of 0.01nm, forces of  $10^{-12}$  N can be detected. Alternatively, the force gradient between probing tip and sample is measured by detecting the frequency shift of the cantilever:

$$\omega'_1 \approx \sqrt{\frac{c_{eff}}{m}} = \sqrt{\frac{c_B - F'}{m}} \quad (1)$$

Where  $\omega'_1$  is the shifted resonance frequency,  $m$  is the mass of the cantilever,  $c_{eff}$  is the effective spring constant. For small force gradients ( $|F'| \ll c_B$ ), the shifted resonance frequency is approximately given by

$$\omega'_1 = \omega_0 \left( 1 - \frac{F'}{2 \cdot c_B} \right) \quad (2)$$

where  $\omega_1$  is the first resonance frequency of the free cantilever. The frequency shift  $\Delta\omega_1 = F'/2c_B$  is then proportional to the force gradient  $F'$ . A repulsive force gradient causes an increase of the resonance frequency whereas an attractive forces gradient  $F' > 0$  causes a decrease of the resonance frequency.

## 1a- Design principles of cantilevers

### i- Thermal vibrations

If we apply the equipartition theorem to the rectangular cantilever with a spring constant  $c_B$ , we get the amplitude ( $\psi_1$ ) of the thermal vibrations of the first eigenmode to be approximately

$$\langle \psi_n \rangle^2 \approx k_B T / c_B \quad (4)$$

which is similar to the simple harmonic oscillator.

For the higher eigenmodes of order  $n$ , we obtain approximately

$$\langle \psi_n \rangle^2 = \frac{k_B T}{c_B} \frac{192}{((2n - 1)\pi)^4} \quad (5)$$

$\langle \psi_n \rangle$  is inversely proportional to  $n^2$ . Consequently, the first eigenmode is dominating. A spring constant of 0.001 N/m results in an amplitude of 6.4 Å. If we apply a repulsive/attractive force to the probing tip the cantilever is stabilized/destabilized and the amplitude  $\langle \psi_1 \rangle$  is reduced/increased significantly. In first approximation the amplitude is

$$\langle \psi_1 \rangle^2 = \frac{k_B T}{1.0302(c_B - 0.9707F')} \frac{k_B T}{c_B - F'} = \frac{k_B T}{c_{eff}} \quad (6)$$

where  $F'$  is the force derivative and  $c_{eff} = c_B - F'$  the effective spring constant. If we assume a repulsive force gradient of 50 N/m, the thermal vibration is reduced from 6.4 Å to about 0.1Å.

### *ii- Resonance frequency*

The first eigenfrequency of the cantilever should be maximized to reduce the influence of ambient vibrations and acoustical perturbations. For a rectangular cantilever, the first eigenfrequency  $\omega_0$  is given by

$$\omega_1 = (1.8751)^2 \frac{t}{l^2} \left( \frac{E}{12\rho} \right)^{1/2} = \frac{(1.8751)^2}{\sqrt{3}} \sqrt{c_B/m} \quad (7)$$

where  $t$  and  $l$  are the thickness and length,  $E$  the Youngs modulus,  $\rho$  the mass density and  $m$  the mass. In order to sustain a high resonance frequency, while reducing the spring constant, it is necessary to reduce the mass of the cantilever. Therefore, the dimensions have to be chosen as small as possible.

## ***1b- Preparation of cantilevers***

Up to now there are two main techniques that are used for the production of levers.

- First, a thin wire or piece of metallic foil is bent and etched electrochemically. As known from the preparation of STM tips a radius of curvature less than 1000 Å can be prepared by this method. The miniaturization of these levers is limited by the manual skill of the experimentalist. Nevertheless, this method is common in the field of magnetic force microscopy where ferromagnetic probing tips are required.

- The second method for cantilever preparation involves microfabrication techniques. Several generations of cantilevers already exist. The first generation is simple cantilevers of rectangular and triangular shape. SiO<sub>2</sub> cantilever are etched out of an oxidized silicon wafer. Standard photo masks are used to define the shape of the levers. With the exception of the cantilever thickness, the geometrical dimensions of length and width are well known and highly reproducible, which facilitates the calibration of the cantilevers. Later, it is shown that the additional measurement of the resonance frequency of the cantilever also gives a reasonable determination of the thickness of the cantilever.

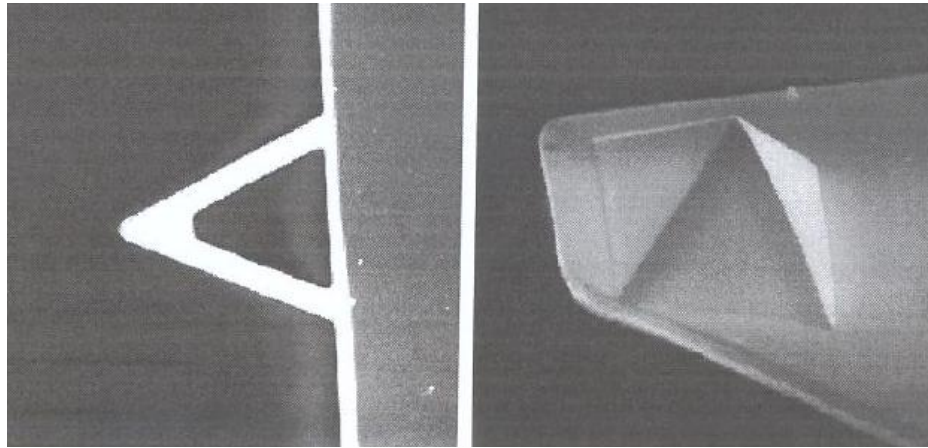


Figure 1- SEM images of a triangular silicon nitride cantilever with integrated probing. Tip height is about 2  $\mu\text{m}$ .

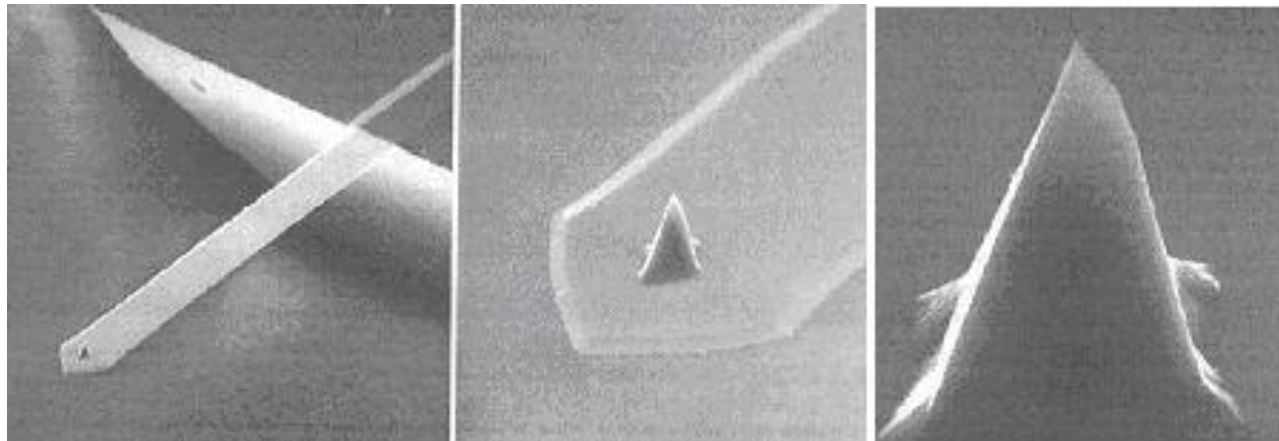


Figure 2- SEM images of a rectangular silicon nitride cantilever with integrated probing. Tip height is about 12.5  $\mu\text{m}$ .

Small fragments of various materials, such as diamond, are glued to the end of these cantilevers, providing a reasonable probing tip as can be shown with scanning electron microscope (SEM) in Figures 1 and 2. For example the end of a diamond piece may be formed by a tetrahedron confined by crystallographic faces.

Some progress has been made in the use of  $\text{Si}_3\text{N}_4$  instead of  $\text{SiO}_2$ .  $\text{Si}_3\text{N}_4$  levers are less fragile and the thickness can be reduced from  $1.5\ \mu\text{m}$  to  $0.3\ \mu\text{m}$ .

## 2- Microscopes

### 2a- Deflection sensors

- Techniques to measure small cantilever deflections

There are different techniques to detect the small displacement of the lever (Fig. 4).

Other sensors incorporate optical interferometry or the reflection of a laser beam from a mirror mounted on the rear side of the lever.

Both setups achieve a vertical resolution of the same order.

Actually, the force sensitivity is already limited by the thermal noise of the cantilever.

Modifications of probing tips are possible (Fig. 3). Depositions of carbon nanotubes or diamond coatings are other possibilities.

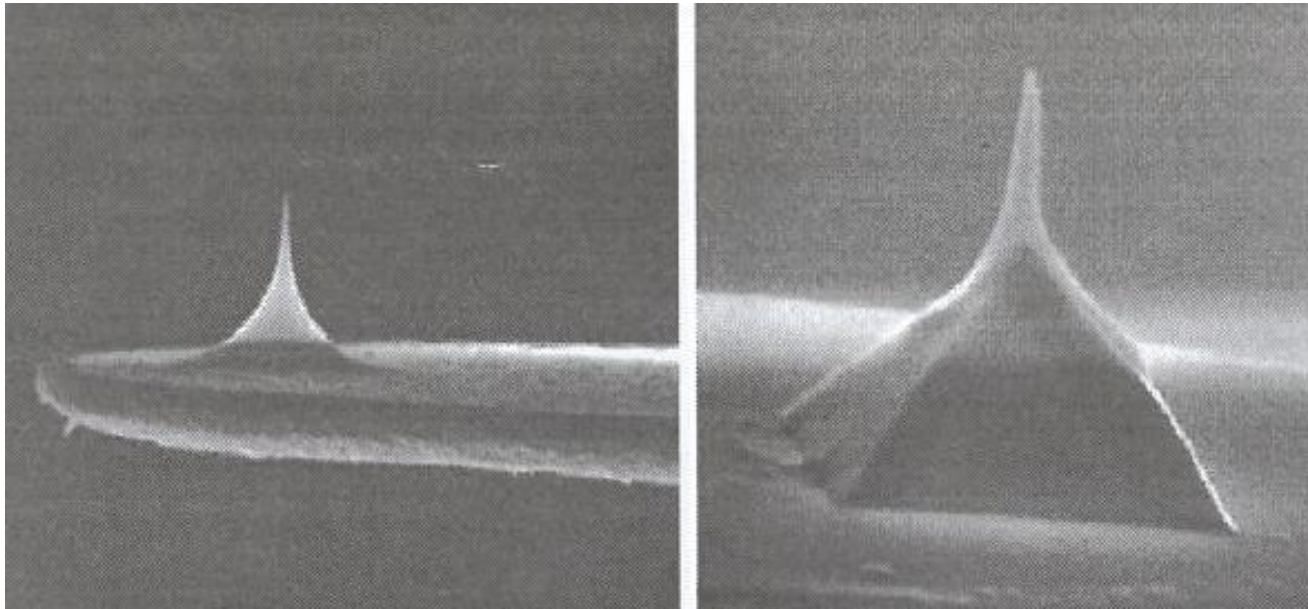


Figure 3- SEM images of modified triangular cantilevers with integrated probing tip: Left, oxidize sharpened. Right, contamination tip deposited with field SEM.

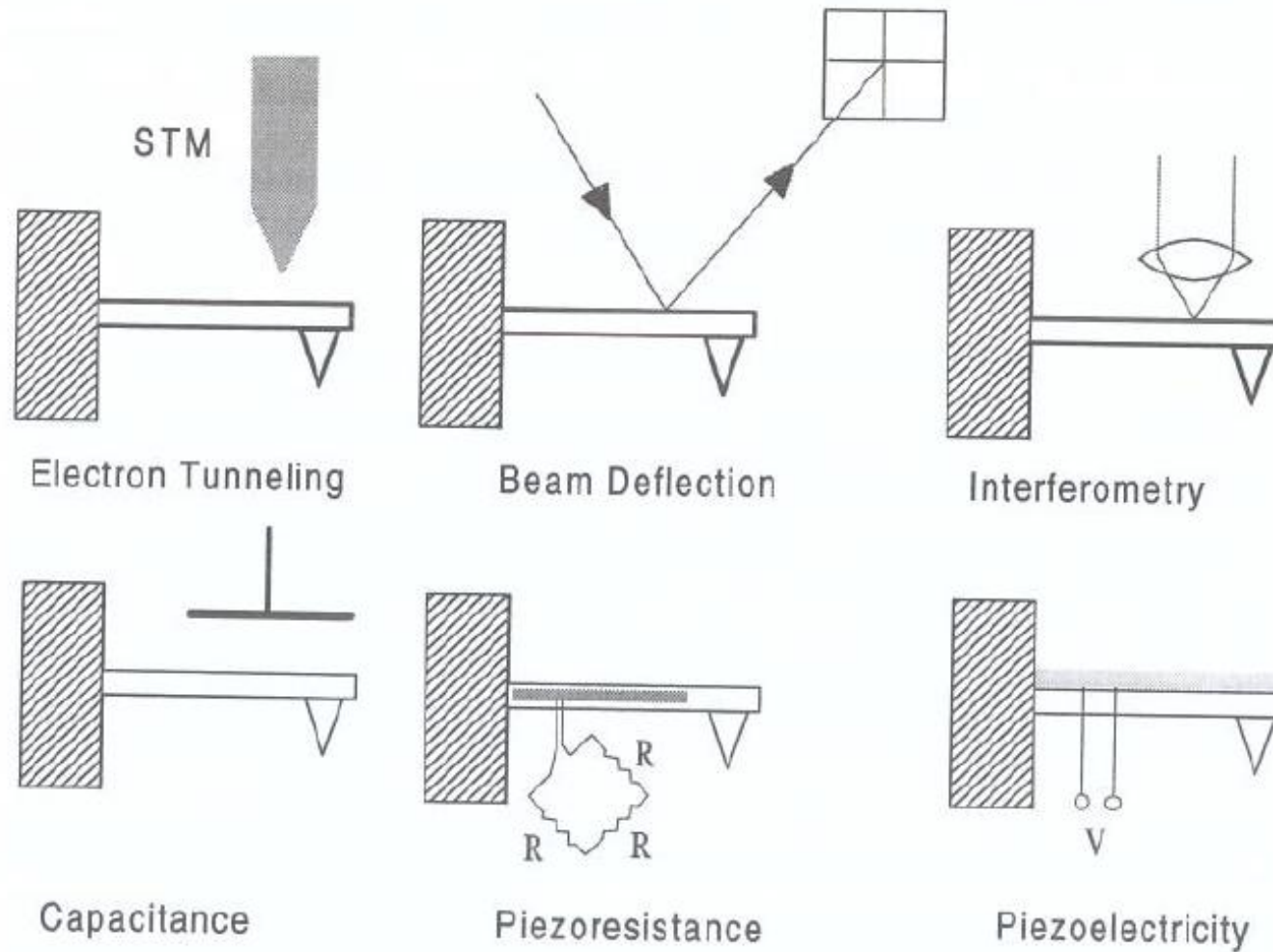


Figure 4- Deflection sensors for scanning force microscope

### ***i- Electron tunneling***

Measuring the tunneling current between the tip and the conductive rear side of the lever is a very sensitive technique.

A decrease in the gap of 1 Å will increase the current by an order of magnitude.

Experimentally a z-resolution of 0.01 Å can be achieved with a bandwidth of few thousand Hz.

Especially high speed scan rates of about 100-1000 Hz per scan line can be performed by digitizing the tunneling current instead of the feed-back output signal.

Due to the high mechanical stability and low thermal drift rates the tunneling SFM can be operated in the dc mode reliable and efficient.

### ***ii- Optical interference (interferometry)***

In 1986 McClelland et al. and Martin et al have presented the first optical interferometers based on homodyne and heterodyne interferometry. The main advantages compared to the tunneling SFM are:

- The interaction between the laser beam and the lever can be neglected.
- Due to the large beam diameter the optical SFM are insensitive to the roughness of the rear side of the lever.

Forces as small as  $10^{-16}$  N could be measured.

Optical SFMs developed towards more stable and compact designs using fiber optical devices or differential interferometers.

## 3- Calibration procedures

### 3a- Calibration of scanner

For both scanning in x- and y-directions and adjusting the z-position with the help of the feed-back loop, piezoelectric elements are used. A voltage is applied across the piezoelectric material. In most cases, the transverse piezoelectric effect is used, which means that the material will extend or contract perpendicular to the applied field  $E$ . The change in length for a simple rod of length  $L$  is given by  $\Delta L = L \cdot |E| \cdot d_{31}$ , where  $d_{31}$  is the piezoelectric coefficient. Scanners have to be designed according to the desired scan range and resonance frequency of the microscope. For low temperature experiments, the reduced sensitivity has to be taken into account. In UHV, the bake-out temperature gives a lower limit for the Curie-temperature. Taking these pre-conditions into account, the piezoelectric elements can be selected. The sensitivity in z-direction for the tube scanner is given by:

$$\Delta z = d_{31} \cdot V \cdot \frac{L}{H} \quad (8)$$

where  $d_{31}$  is the piezoelectric coefficient (for PZT-5H  $d_{31} = -2.62 \text{ \AA/V}$ ).

The deflection in x-direction (y-direction is analogous) is given by

$$\Delta x = \frac{L^2}{2 \cdot R} = 2 \cdot \sqrt{2} d_{31} \cdot V \cdot \frac{L^2}{\pi \cdot D \cdot H} \quad (9)$$

where  $R = \pi D H / [4(2)^{1/2} d_{31} V]$  is the curvature of bending. Usually, the x-sensitivity is defined by

$$s_x = \Delta x / V = 2 \cdot \sqrt{2} d_{31} \cdot \frac{L^2}{\pi \cdot D \cdot H} \quad (10)$$

Thus, a PZT-5H scanner with a diameter of  $D = 12.7$  mm, a wall thickness of  $H = 1$  mm and a length of  $L = 12.7$  mm gives a sensitivity of  $30 \text{ \AA/V}$ . The sensitivity is reduced by a factor of two when the voltage is applied only to one quadrant.

Material Properties	PZT-5A	PZT-5H	PZT-8
$D_{31}$ (Å/V)	-1.71	-2.62	-0.95
$D_{33}$ (Å/V)	3.80	5.83	2.20
Dielectric Constant	1725	345	1050
Curie temperature (°C)	350	190	300
Mechanical Q	100	65	960

Table 1- Properties of PZT materials

### **3b- Calibration of lateral forces**

Manufacturer's data are usually not sufficient and can lead to errors of up to a factor 10. Thus, each cantilever has to be characterized.

One way is to use an electron microscope and to determine all the relevant parameters, such as: Tip radius R; height of tip h ; width, thickness and length of cantilever (w, t, l) and position of tip on the cantilever.

In addition, elastic constants are needed: Young's modulus E, shear modulus G. Having determined all these parameters, the normal spring constant  $c_B$  and the torsion spring constant  $c_t$  for a rectangular cantilever are given by equations above where E is the Young's modulus and  $G = E/[2(1 + \nu)]$ .

$$c_B = \frac{E \cdot w \cdot t^3}{4 \cdot l^3} \quad (11)$$

$$c_t = \frac{G \cdot w \cdot t^3}{3 \cdot h^2 \cdot l} \quad (12)$$

For commercially available silicon cantilevers, the elastic properties are well-defined and the first resonance frequency in normal direction  $f_1 = \omega_1/2\pi$  can be used to determine the thickness of the cantilever more accurately:

$$t = \frac{2 \cdot \sqrt{12}\pi}{1.875104^2} \sqrt{\frac{\rho}{E}} f_1 \cdot l^2 = 7.23 \times 10^{-4} \text{ s/m} \cdot f_1 \cdot l^2 \quad (13)$$

where  $\rho$  is the density of the cantilever, for silicon cantilevers  $\rho = 2.33 \times 10^3 \text{ kg/m}^3$  and  $E = 1.69 \times 10^{11} \text{ N/m}^2$ ).

Thus, the procedure is more simplified: The lateral dimensions of width and length ( $w, l$ ) can be determined with an optical microscope.

Usually, these dimensions are quite reproducible by current microfabrication procedures. The height of the tip  $h$  can vary a few microns and should be checked with an optical or electron microscope.

## **4- Modes of operation**

### ***4a- Imaging modes***

#### ***i- Equiforce mode:***

In principle the equiforce mode is the most important mode being the easiest to interpret. During the scan process the deflection of the lever and therefore the force is kept constant by the feed-back loop. This mode is the most important mode for contact mode AFM.

#### ***ii- Variable deflection mode:***

The feed-back is disabled. During the scan process the deflections are measured by the detector.

If the relative variations of the force are not too large this mode can be interpreted in a similar manner as with the equiforce mode.

In contrast to the equiforce mode, higher scan rates can be achieved, because the feed-back has not to be used.

#### ***iii- Constant frequency mode:***

The cantilever is excited close or at the resonance frequency. During lateral scanning, the frequency of the cantilever is kept constant.

Typically, the cantilever is operated in a non-contact regime or near-contact regime.

#### ***iv- Tapping mode:***

The cantilever is excited close or at the resonance frequency. During lateral scanning, the amplitude is kept constant.

The oscillation amplitudes are rather large ( $>10\text{nm}$ ) and the tip gets into contact during part of the oscillation cycle.

Thus, dissipative processes may be present, but are usually not observable in the lateral force signal.

The phase difference between excitation signal and lever oscillation is measured. This phase difference is related to local variations of the viscosity.

#### ***v- Spectroscopic mode:***

Being common in STM, are not so far developed in SFM. One example has been given by Mate et al [J. Chem. Phys. **94**, 8420 (1991)]. The authors performed spatially resolved force-distance curves on a liquid polymer determining not only capillary forces but also the thickness variations of the liquid film.

Properties, such as adhesion, local compliance, viscosity or friction can be investigated as a function of properties, such as normal force, velocity or scan direction.

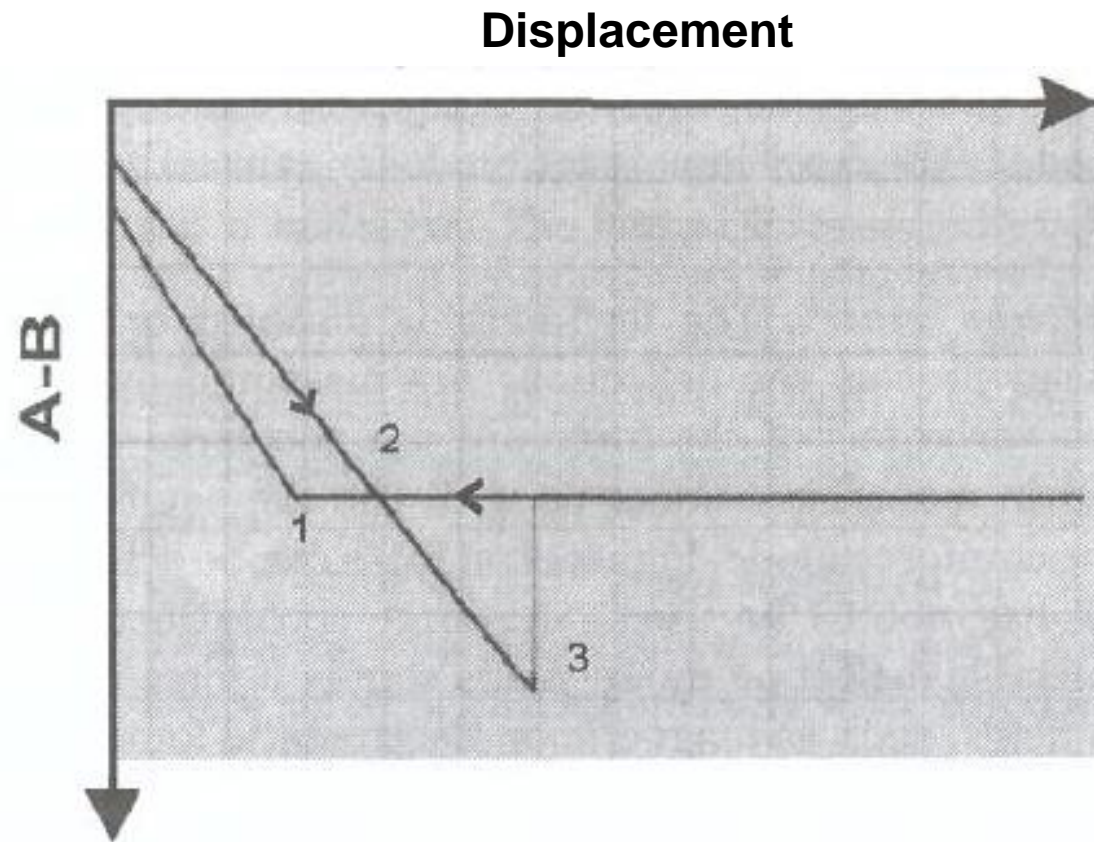


Figure 5- The normal deflection A - B is plotted vs. the sample movement  $z_s$ . Due to the low spring constant instability occurs.

## 4b- Force vs. distance curves

SFM measure the force as a function of distance between tip and sample.

Figure 5 shows a experimental  $z_t(z_s)$ -plots measured in dried nitrogen and contains information about the interaction between sample (oxidized silicon) and tip (silicon).  $z_s$  is the movement of the sample and  $z_t$  is of the lever and tip.

Both movements are approximately perpendicular to the sample surface.

Multiplicating  $z_t$  with the spring constant  $c_B$  the force  $F = c_B \cdot z_t$  can determined.

Neglecting elastic deformations of the sample and tip the interaction distance between tip and sample  $d$  is given by  $d = z_t - z_s$ .

When the sample is approached towards the probing tip the lever bends due to the attractive force.

At point 1 the gradient of the attractive force surpasses the spring constant  $c$  which leads to a first point of instability.

The level of zero net force is passed, which means that the attractive and repulsive force cancel each other. In the repulsive regime the sample just pushes the lever.

The sample is retracted again point 2 is passed.

The maximum attractive force (adhesive force or pull-off force) is reached (point 3) where a second instability occurs and the tip jumps out of contact. Finally, we reach again the free lever (no measurable interaction between tip and sample).

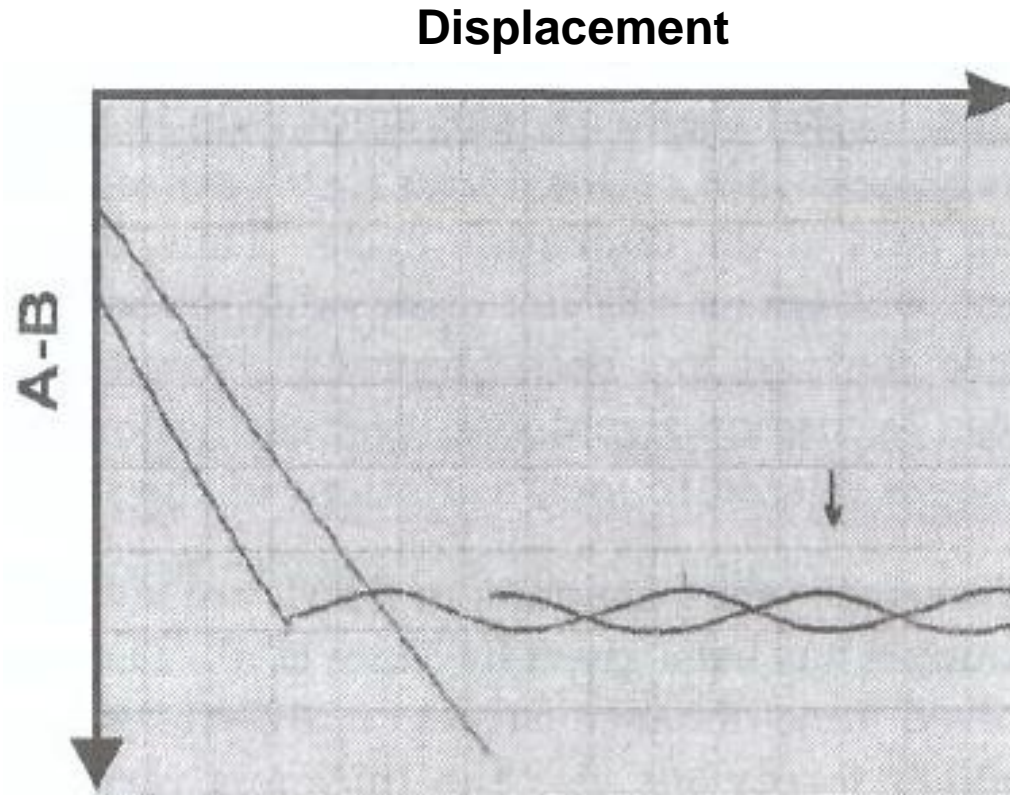


Figure 6- Same as Fig. 5, but with bad focus, which leads to interference effects between the beam reflected from the sample and the beam reflected from the cantilever.

From this plot we can determine parameters such as the pull-off force, which is also called adhesion.

Several phenomena such as capillary forces, tip shape and piezo creep effects impede a more quantitative determination of the interaction under ambient conditions.

Weisenhorn et al [Appl. Phys. Lett. **54**, 2651 (1989)] could actually demonstrate the influence of capillary forces by comparing  $z_t(z_s)$ -plots in air and water. If the lever was fully immersed into water capillary forces can be excluded. A significantly decreased pull-off force of  $10^{-9}$  N in water compared to  $10^{-8}$  to  $10^{-7}$  in air has been observed. Furthermore, piezo creep effects can be minimized with faster acquisition cycles or actively corrected z-piezos (e.g., with capacitance detectors).

Figure 6 shows a  $z_t(z_s)$ -plots, where the focus was not optimized. Here, interference between the laser beam reflected from the sample and the beam reflected from the cantilever occurs. The distance between the interference maxima,  $d_{\max} = \lambda/\sin\theta$  is related to the wavelength of the laser source,  $\lambda$  (typically about 620 nm), where the angle of incidence of the laser beam relative to the sample surface,  $\theta$  is taken into account.

The focus was rather bad ( $>30 \mu\text{m}$ ), which caused interference patterns, which are pronounced in the FFM image.